Distribution Agreement

In presenting this thesis as a partial fulfillment of the requirements for a degree from Emory University, I hereby grant to Emory University and its agents the non-exclusive license to archive, make accessible, and display my thesis in whole or in part in all forms of media, now or hereafter now, including display on the World Wide Web. I understand that I may select some access restrictions as part of the online submission of this thesis. I retain all ownership rights to the copyright of the thesis. I also retain the right to use in future works (such as articles or books) all or part of this thesis.

Yu Zhang April 9, 2019

Molecular Cloning and Functional Characterization of the CBX7 Transcript Variant Gene

by

Yu Zhang

Young-sup Yoon, MD, Ph.D.
Adviser

Department of Biology

Young-sup Yoon, MD, Ph.D.

Adviser

Kathleen Campbell, Ph.D.

Committee Member

William G. Kelly, Ph.D.

Committee Member

2019

Molecular Cloning and Functional Characterization of the CBX7 Transcript Variant Gene

By

Yu Zhang

Young-sup Yoon, MD, Ph.D.

Adviser

An abstract of
a thesis submitted to the Faculty of Emory College of Arts and Sciences
of Emory University in partial fulfillment
of the requirements of the degree of
Bachelor of Sciences with Honors

Department of Biology

2019

Abstract

Molecular Cloning and Functional Characterization of the CBX7 Transcript Variant Gene
By Yu Zhang

Polycomb group proteins (PcG) are epigenetic regulators that modify chromatin structures and control gene expressions. They play critical roles in cellular proliferation and associated with cancers. CBX7, a subunit of PcG, has been previously identified to play two opposing roles: a tumor suppressor and an oncogene. Regarding this discrepancy, it was suggested that the function of CBX7 could be tissue- and context-specific. In this study, we identified the *Cbx7* variant gene that may possibly explain the discrepancy of CBX7 functions. We successfully cloned *Cbx7* variant gene via TA cloning. The sequencing result indicated that the *Cbx7* and the variant gene have different exon 5 region. Based on this data, we hypothesized that the *Cbx7* variant gene that contains the extra exon 5 region is the controlling factor in whether the *Cbx7* gene become an oncogene or tumor suppressor. For the gain of function (GOF) analyses, we constructed recombinant adenovirus that overexpresses CBX7 and its variant protein. These adenoviral particles were used to infect the mouse embryonic fibroblasts (MEF). To validate and characterize GOF effects, we performed quantitative real-time PCR to check mRNA expression, Western blot to verify the protein expression, and MTT assay to indirectly assess cell proliferation rate. Understanding the mechanisms underlying the discrepancy on CBX7 function will grant scientists a clearer understanding of its function and will assist in the development of future studies regarding developmental biology, cancer treatment, and tissue regeneration.

Molecular Cloning and Functional Characterization of the CBX7 Transcript Variant Gene

By

Yu Zhang

Young-sup Yoon, MD, Ph.D.

Adviser

A thesis submitted to the Faculty of Emory College of Arts and Sciences
of Emory University in partial fulfillment
of the requirements of the degree of
Bachelor of Sciences with Honors

Department of Biology

2019

Acknowledgements

I would like to thank everyone has helped me with this project and my undergraduate career.

Dr. Yoon has also been an integral part of my career. I appreciate being welcomed into his lab with open arms and an opportunity to perform scientific research. His advising has also helped to shape my career path.

Dr. Campbell was one of my first professors at Emory University. She helped to convince me that I truly love biology. The opportunity to tutor students underneath her has been an amazing opportunity while at Emory.

Dr. Kelly taught one of my favorite courses at Emory University. I was passionate about biochemistry, and his course has well prepared me to understand many complicated biological mechanisms.

I would especially like to thank Dr. Kyuwon Cho for all of his hard work in helping to develop this project and for taking me on as a student, since he helped and taught along every step of the way.

Table of Contents

Introduction

Epigenetic contribution to cancer formation

Cancer is a fatal disease in which cells continue to quickly grow and divide while acquiring different characteristics in a progressive manner. It is mostly caused by mutations, amplifications or deletions of specific genes (1,2). Epigenetic modifications also contribute to the acquisition of tumorigenic phenotypes (3). In different types of cancer, various epigenetic mechanisms can be disturbed, such as silencing of tumor suppressor genes and activation of oncogenes through changing methylation patterns (4,5). DNA hypermethylation is one of the most common epigenetics mutations, which can silence tumor suppressor gene and allow cells to grow and reproduce uncontrollably. It can lead to tumorigenesis and cancer initiation. For example, cyclin-dependent kinase inhibitor p16, a cell-cycle inhibitor, can be silenced due to promoter hypermethylation (5). In addition, DNA hypomethylation of growth promotor gene can also result in different types of cancers such as gastric cancer and melanoma through increasing genomic instability (6). Therefore, epigenetics regulators such as polycomb group (PcG) proteins, methyltransferases and chromatin-remodeling enzymes serve a crucial role in charge of regulating epigenetic changes to prevent cancer development and progression (7).

Polycomb-group proteins, epigenetic regulators

As first discovered in fruit flies, PcG proteins are a class of key epigenetic regulators and have been implicated in cellular proliferation and cancer development. This class of epigenetic regulators includes BMI-1, EZH2, and SUZ12. BMI-1 has a strong association with the development of cancer (12). As it was first discovered, mutations in BMI-1 were found to be able to facilitate lymphomagenesis (12). BMI-1 can also lead to tumorigenesis in mice. The reason why BMI-1 has these functional characteristics is because it can downregulate transcription and

can target the Ink4a/Arf locus, which is a tumor suppressor locus (13). This gene locus controls senescence and apoptosis of cells and interacts with other tumor suppressors such as Rb and p53 (14). Finally, other PcG proteins such as EZH2 and SUZ12 also have similar tumorigenesis capacity as BMI-1. *EZH2* is a histone methyltransferase that catalyzes tri-methylation of histone H3 at Lys 27 (H3K27me3) to regulate gene expression (15). *SUZ12* is also needed for the histone methyltransferase activity and lead to efficient H3K27 methylation (16). Unregulated EZH2 activity and high *SUZ12* expression are associated with metastasis of *tumor (15,16).*

PcG-encoded proteins are assembled into two distinct Polycomb Repressive Complexes (PRC) termed PRC1 and PRC2 (17). The interaction of PRC1 and PRC2 with the genome is shown in Figure 1 (18).

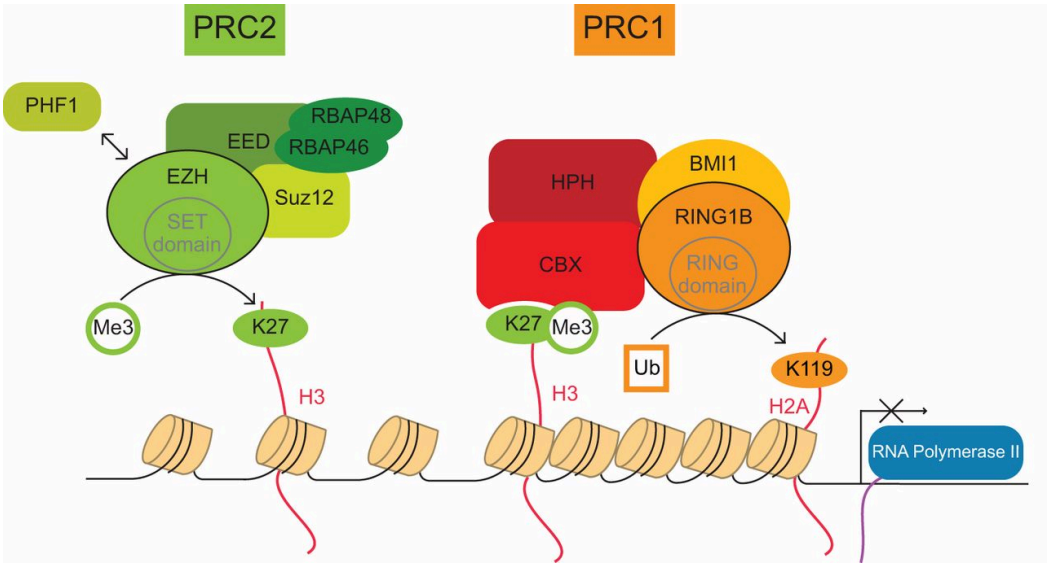

Figure 1: Polycomb-repressive complexes (PRCs) and their enzymatic activities. The PcG transcriptional repressors are organized in two main PRCs, PRC1 and PRC2. Both complexes consist of many enzymatic subunits. They interact with genome to silence the gene expression.

PRC1 and PRC2 were found to be able to silence the gene expression that can causally link to tumorigenesis (18). PRC2 can facilitate the methylation of histone H3 at lysine 27 (19). This methylation modification creates a binding site, and PRC1 binding can contribute to gene silencing by limiting the access of chromatin to transcription factors.

Chromobox family proteins

Chromobox (CBX) family proteins are canonical components in PRC1(20). There are at least eight different types of CBX protein. They participate in the regulation of heterochromatin and gene expression. They can transcriptionally repress target genes via chromatin modification (21). Several studies have highlighted the functional specifications among CBX family members in various cancers, including lung, colon, and breast cancer (20,21,22).

Among CBX family members, CBX7 is one of the most important chromobox family proteins because CBX7 is highly associated with different types of cancer (23). However, its role in cell proliferation is controversial. A number of groups reported that CBX7 is an oncogene and its expression levels significantly correlated with aggressive tumors (24,25). A study showed that CBX7 extends the lifespan of a wide range of normal human cells and immortalizes mouse fibroblasts (26). A few studies also indicated that CBX7 expression levels were increased in thyroid, colorectal, breast, pancreas and glioblastoma (27,28,29). In short, CBX7 can lead to various cancer development.

On the other hand, other studies claim that CBX7 is a tumor suppressor gene. One of the studies indicates that low CBX7 protein expression in human lung carcinomas has a strong correlation with CCNE1 overexpression (30). In addition, the tumor suppressor role of CBX7 has been also confirmed with Cbx7-null mice (24). Several studies have indicated that CBX7

expression can reduce the growth rate of various tumors by inhibiting signaling pathways (31,32,33).

Despite substantial number of studies on CBX7, there is still a huge discrepancy in the reality of CBX7 function. The question remains whether *Cbx7* is an oncogene or a tumor suppressor gene. Regarding this discrepancy, it was suggested that the function of CBX7 could be tissue and context specific. However, the mechanism whereby CBX7 plays specific roles is unclear.

To address the issue, targeted Cbx7 mRNA was isolated from an embryonic mouse heart and then its cDNA was generated. During the process, a *Cbx7* variant gene was identified that may possibly explain the discrepancy of functions of CBX7. We hypothesized that CBX7 and its variant play two opposing roles in cell proliferation. The *Cbx7* variant gene was successfully cloned via TA cloning, and the sequencing result indicated that *Cbx7* and its variant gene have different exon 5 regions. For the gain of function (GOF) analyses, recombinant adenovirus was constructed to infect Mouse Embryonic Fibroblasts (MEFs) so *Cbx7* and its variant gene could be overexpressed. To validate and characterize GOF effects, we performed a quantitative real-time PCR to test cell cycle marker expression, western blot to verify the protein expression, and 3-(4,5-Dimethylthiazol-2-yl)-2,5-diphenyltetrazolium bromidefor (MTT) assay to indirectly confirm cell proliferation. This study identified a transcript variant of Cbx7 and further study may offer insights into mechanism how the *Cbx7* gene has two opposite functions as a tumor suppressor and an oncogene.

Material and Methods

Isolation and Amplification of *Cbx7* gene

Targeted *Cbx7* mRNA was isolated from the newborn fetal mouse heart. By using reverse transcriptase, its cDNA was generated. Two pairs of primers derived from the nucleotide sequence

of the *Cbx7* gene were used to amplify cDNA fragments. The PCR reaction was carried out to amplify *Cbx7* gene. During the process, we detected a gene right above the *Cbx7* gene. This new gene was named the *Cbx7* variant gene, and all cDNA material was collected for the cloning step.

TA cloning

TA cloning relies on the ability of adenine (A) and thymine (T) on different DNA fragments to hybridize together (Fig 2). Taq polymerase was used to add a single deoxyadenosine (A) to the 3'-end of the *Cbx7* variant gene. The *Cbx7* variant gene with the adenine overhang was paired with thymine and ligated into TA cloning pCR2.1 TOPO vector. The vector was then inserted into *Escherichia coli* (*E.coli*) which was viable for transformation. To confirm the insertion, a restriction enzyme called EcoR1 was used to digest pCR2.1 TOPO plasmid.

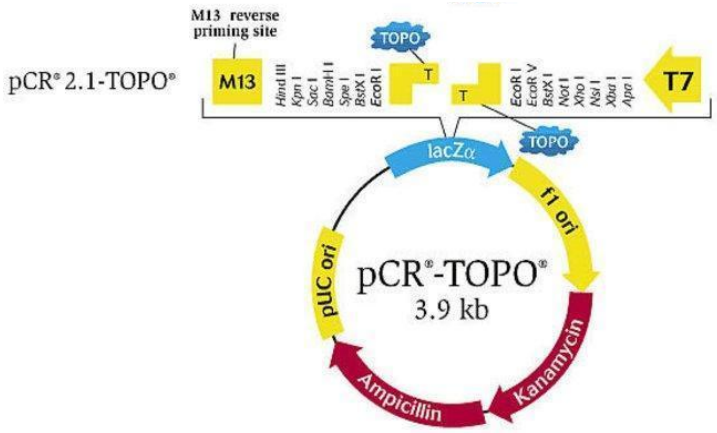

Figure 2. TA cloning plasmid. the *Cbx7* variant gene was ligated to pCR2.1-TOPO plasmid for cloning in order to amplify the DNA construct.

The Blue-White Screening

The blue-white screening was also carried out to verify the insertion. *E.coli* was then grown in the presence of 5-bromo-4-chloro-3-indolyl-β-D-galactopyranoside (X-gal). Cells transformed with DNA containing the *Cbx7* variant produced white colonies; Whereas cells transformed with

only the vector produced blue colonies. The results showed some white colonies, which indicated the insertion of *Cbx7* was successful.

Sequencing

The *Cbx7* variant gene was sent off to be sequenced. The sequencing result was then analyzed and compared to the *Cbx7* gene.

Cell Culture

Two types of cell lines were used: HEK-293 cells and MEF cells. HEK293 were used for virus amplification and titration. MEF cells were used for conducting western blot, Colorimetric 3-[4,5-dimethylthiazole-2-yl]-2,5-diphenyltetrazolium bromide (MTT) assay, and Real-time polymerase chain reaction (rtPCR). These two cell lines were both maintained and incubated in high glucose Dulbecco's Modified Eagle Medium (DMEM) supplemented with 10% Fetal Bovine Serum (FBS), Horse serum, Non-Essential Amino Acids (NEAA) and Glutamax. For the MTT assay, half of the MEF cells were incubated with 2% FBS media. The other half of the MEF cells were incubated with the original 10% FBS media.

Generating Recombinant Adenovirus

HEK-293 cells were transfected with the recombinant adenoviral plasmids to generate recombinant. The empty adenovirus was named: ad-Mock. *Cbx7* recombinant adenovirus was named as ad-Cbx7, and *Cbx7* variant recombinant adenovirus was named as ad-Cbx7 V. Ad-Mock was the control group. Ad-Cbx7 and Ad-Cbx7 V were the experimental groups. In order to obtain a large amount of virus, the 293 cells that contained virus particles were collected in a 50ml tube and centrifuged at 1,500 rpm for 5 min. The supernatant was transferred to a new 50ml tube and kept at 4C degree. The cell pellet was lysed during the freezing/thawing procedure 3 times. 0.5 ml or 1ml of PBS was added to the lysed cell solution and transferred to microtubes, which were then centrifuged at 13,000 rpm for 5 min. After centrifugation, the upper fraction, which is the virus

layer, was transferred to new microtubes and stored at 4 degrees for the next adenovirus amplification. After these three different groups of adenoviruses were amplified, we performed adenovirus titration to measure the concentration of newly amplified adenovirus. First, HEK 293 cell were plated in P100 dish at 50-70% confluency and incubated overnight for attachment. The cell condition was checked under the microscope. 293 cells were subcultured into three 12-well plates. Once confluency reached 70%, the titration procedures were started. The designated amount of viral solution was delivered to each well of the 12-well plates. After three 12-well plates were treated with virus, these plates were then incubated for 48 hours. After incubation, the result of titration was evaluated and recorded. We then waited for 48 hours and then recorded the cell condition under a 2X microscope.

Western Blot

Equal concentrations of recombinant adenovirus were seeded to infect Mouse Embryonic Fibroblasts (MEF) cells separately, so three MEF cell plates were used: ad-Mock plate, ad-CBX7 plate, and ad-CBX7V plate. After infecting MEF cells, we extracted and quantified protein fraction from each MEF cells plate through the bicinchoninic acid (BCA) assay. These proteins were used in the western blot to check for the expression of CBX7 variant protein, as compared to the expression levels of Mock, and CBX7 variant protein. For western blot analysis, proteins were extracted and separated by SDS-PAGE and transferred onto PVDF membranes. Proteins were probed with antibodies against CBX7 or actin B1. Proteins of interest were detected with HRP-conjugated rabbit anti-mouse IgG antibodies and visualized with the Pierce ECL western blotting substrate (Thermo Scientific, Rockford, IL), according to the provided protocol.

Colorimetric MTT Assay

Next, we tested whether the *Cbx7* variant gene leads to a change in cell proliferation level by performing 3-(4,5-Dimethylthiazol-2-yl)-2,5-diphenyltetrazolium bromidefor (MTT) assay,

which checks cellular oxidoreductase enzyme levels that reflect the number of viable cells present. The MTT assay was conducted in two media conditions: 10% FBS media condition and 2% FBS media condition. By testing cell proliferation in different media conditions, we could better distinguish whether MEF cell proliferation is caused by the *Cbx7* variant gene or by the richness of the medium.

Real-time Polymerase Chain Reaction

Real-time PCR (rt-PCR) was conducted to check proliferation markers such as cyclins (ccn), Cyclin-dependent kinase inhibitor 2A (p16), and tumor suppressor ARF. Cyclins are eukaryotic proteins that play an active role in controlling nuclear cell division cycles and regulating cyclin-dependent kinases (CDK) (34). There are two main groups of cyclins, G1/S cyclins, which are essential for the control of the cell cycle at the G1/S (synthesis) transition, and G2/M cyclins, which are essential for control of the cell cycle at the G2/M (mitosis) transition (35,36). P16 plays an important role in cell cycle regulation by decelerating the cell's progression from G1 phase to S phase, and therefore acts as a tumor suppressor that is implicated in the prevention of cancer (37). ARF is involved in cell cycle regulation. Thus, it inactivates certain cyclin-CDK complexes and leads to decreased transcription of genes that would carry the cell through the G1/S checkpoint of the cell cycle. Checking proliferation markers could provide direct evidence of cell proliferation. The first step before performing rt-PCR was to collect targeted RNA. Total RNA was extracted using the RNeasy minikit (Qiagen) and quantified. Then, equal amounts were used for generating cDNAs using Superscript II (Gibco) together with oligo-dT primers. After reverse transcription, serial dilutions of the first-strand of cDNA were used for PCR reactions with specific primers. The resulting amplified products were resolved on 2% agarose gels and quantified. The reference gene used for normalization was *Gapdh*, a well-known housekeeping gene.

Results

An additional transcript for mouse Cbx7 gene was detected

In our unpublished previous study, we detected an additional band for CBX7 with higher molecular weight in the fetal mouse heart via western blot (Data not shown). We assumed that the additional band could represent a transcript variant for CBX7. To explore the possibility, we isolated mRNA from fetal mouse heart and converted it to cDNA. We designed primers that can amplify the full length CBX7 gene. A PCR reaction for Cbx7 showed that there was a band right above the band corresponding to *Cbx7* cDNA (Fig.3). This higher band indicated a larger sequence size than *Cbx7*, approximately 1000 bp. This gene was named the *Cbx7* variant gene. In order to further study this variant gene, TA cloning was conducted to amplify and sequence the *Cbx7* variant gene.

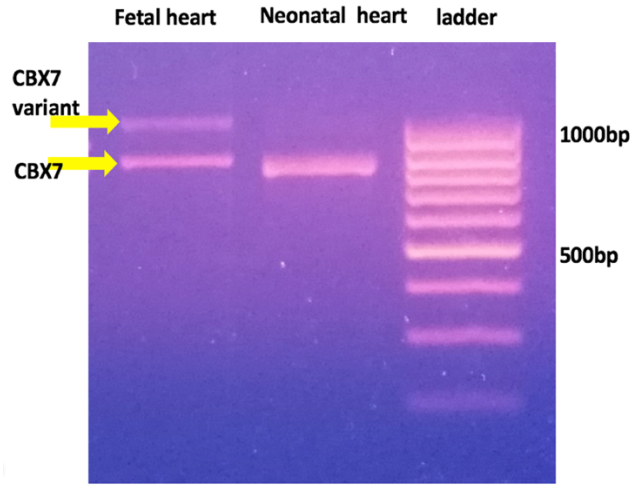

Figure 3. PCR result of the *Cbx7* and variant gene from fetal and neonatal mouse hearts. The *Cbx7* variant gene traveled a shorter distance into the gel than *Cbx7* gene which meant it had more base pairs than the *Cbx7* variant gene

The Cbx7 variant gene was successfully inserted into TA cloning plasmid

The *Cbx7* variant gene was ligated into the TA cloning pCR2.1 TOPO vector. The vector was then inserted into *Escherichia coli (E.coli)* which was viable for transformation. *E.coli* are grown in the presence of X-gal. Cells transformed with vectors containing *Cbx7* variant produced white colonies; cells transformed with only the vector were blue. Our results showed there were some white colonies which meant insertion of *Cbx7* was successful (Fig.4).

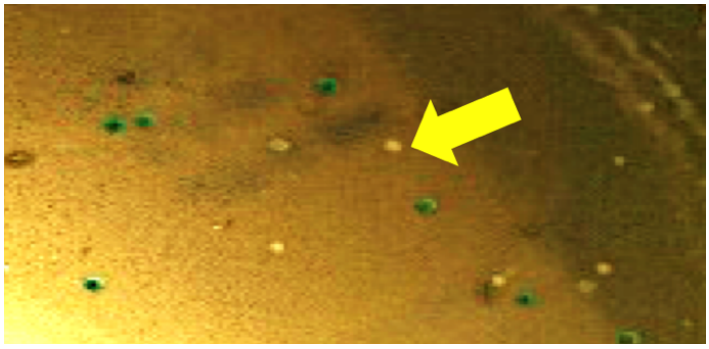

Figure 4. The result of the Blue-White screening. The yellow arrow indicates white colonies that contain cells that were transformed with vectors contain *cbx7* variant gene. Cells transformed with non-recombinant plasmids produced blue colonies

To check the insertion, we used a restriction enzyme called EcoR1 to digest the pCR2.1 TOPO plasmid. The result showed predominately two sizes of bands on the gel: one at 1000bp and the other at 500bp (Fig 5.). The 1000bp band corresponds to plasmid and the 500bp to the *Cbx7* variant genes. The bands in column 1 and column 7 were below 500bp. It was possible that they were the *Cbx7* gene.

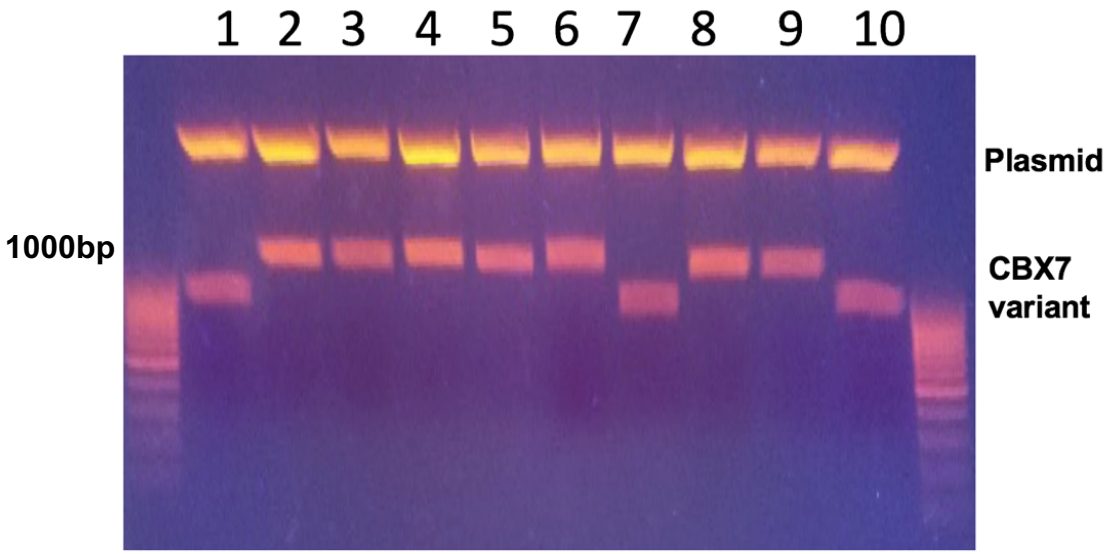

Figure 5. Restriction enzyme digestion of pCR2.1-TOPO plasmid. DNA from ten colonies were analyzed. The upper bands corresponded to pCR2.1-TOPO plasmid. The lower bands correspond to inserted DNA.

Cbx7 variant gene was sequenced

Cbx7 variant gene was sent to be sequenced by the sequencing company (Genewiz). The sequencing result showed that the *Cbx7* variant gene has a longer exon 5 region than *Cbx7*(Fig.6). This extra exon 5 might contribute to a new property of the variant gene. Therefore, further investigation of the variant gene function was needed. In order to effectively delivery the gene to target cells, three types of recombinant adenovirus were constructed: Ad-Mock, Ad-Cbx7, and Ad-Cbx7 V. To measure their viral concentration, titration was performed.

Figure 6. Aligned protein sequence result of the *Cbx7* variant gene and *Cbx7* gene. The CBX7 protein sequence was shorter than its variant gene protein sequences. Their regions of exon number 5 were also different.

Three types of recombinant adenovirus *were titrated*

All virus titration was performed in a 12-well plate. Three 12-well plates were used to conduct titration for ad-Cbx7, ad-Cbx7 V and ad-Mock separately (Fig. 7,8,9). Serial dilution was used to dilute viral concentration. Under the 2X microscope, the titration results of ad-Cbx7 had shown the first well of the 12-well plate had the highest amount of adenovirus. The survival rate of HEK 293 cells were 0% (Fig. 7). After rating the survival rate for all 12 wells, the 7th well was the starting point of having 90% or higher survival rate of HEK 293 cells (Fig. 7). This means that cells could tolerate the infection or gene delivery process by the amount of virus in the 7th well.

The same rating system was used for Ad-Cbx7 and Ad-Mock plates. The 9th well on the ad-Cbx7 plate and the 10th well on the ad-Mock plate indicated 90% or higher survival rate of HEK 293 cells (Fig.8, 9). The titration procedure helped equalize the viral concentration. Therefore, equal concentrations of Ad-Mock, Ad-Cbx7 and Ad-Cbx7V were used to perform western blot to check protein expression of each gene.

Figure 7. Titration results of CBX7 variant recombinant adenovirus. Cells were mostly dead in the first and second well. As the amount of virus decreased, cell survival rate was about 90% from the fifth well.

Figure 8. Titration results of CBX7 recombinant adenovirus. Cells were mostly dead in the first row. As the amount of virus decreased, cell survival rate was about 90% from the fifth well.

Figure 9. Titration results of Mock recombinant adenovirus. Cells were mostly dead in the first and second row. As the amount of virus decreased, from the ninth well cell curvival rate was about 90%.

The western blot analysis indicates different protein expression level of CBX7 and its variant

To check the protein expression level, western blot was performed after infecting MEF cells with Ad-Mock, Ad-Cbx7, and Ad-Cbx7V. β actin antibody was the positive control group which presented equal protein expression for all three types of adenovirus (Fig.10). However, the protein size and expression level of CBX7 and CBX7 variant proteins were different which was detected by using the Cbx7 antibody. The size of the CBX7 variant protein was 35 kDa. The size of the CBX7 protein was 20 ka (Fig.10). As Ad-CBXV level decreased, the band also became weaker. However, as Ad-CBX level decreased, the bands didn't change the strength (Fig.10).

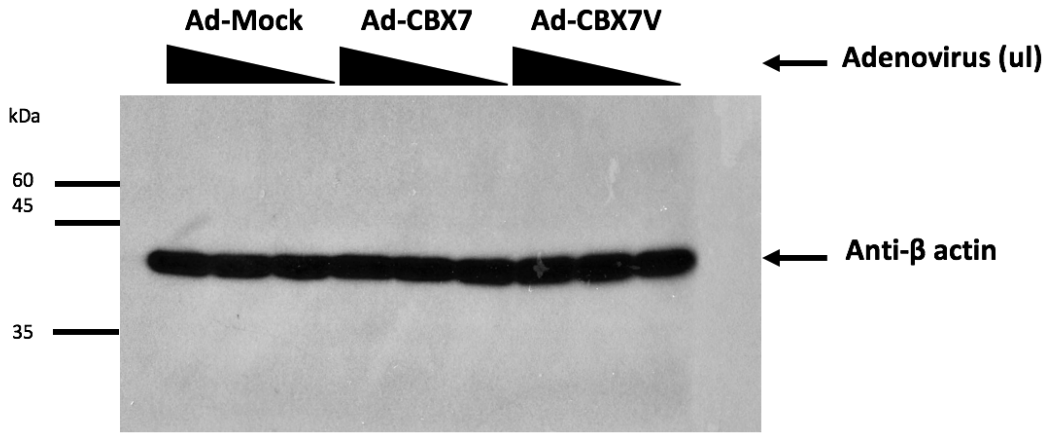

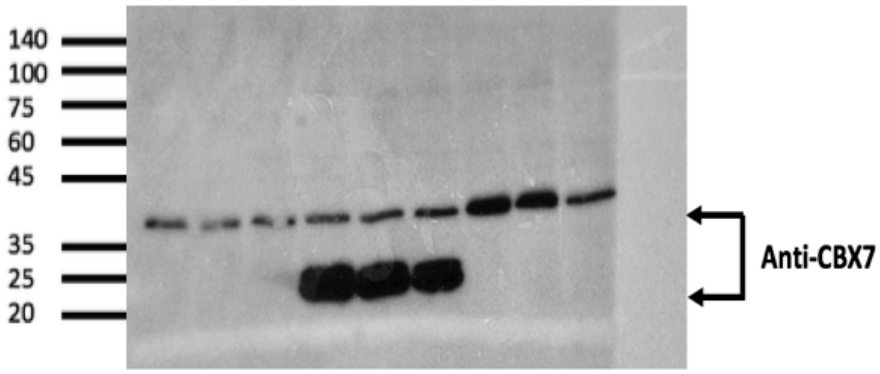

Figure 10. western blot results of CBX7 and its variant protein. CBX7 antibody detected both CBX7 and CBX7 variant proteins. β actin antibody was the control group that detected Mock, CBX7, and CB7 variant proteins.

MTT Assay indicated MEF cell proliferation level

To investigate the proliferative potential of the *Cbx7* variant gene, MTT assay was conducted by interactively measuring mitochondria concentration. As cell proliferate, the number of mitochondria would also increase. One possible confounding factor was the nutritional level of the media. Highly nutritious media would enable MEF cells to proliferate more. To experimentally exclude this confounding variable, MEF cells were incubated in two conditions: 10% FBS and 2% FBS media. 10% FBS media has more nutritious media than 2% FBS media. First MTT assay was conducted with 10%FBS. No treatment group was a negative control group. The MTT assay result indicated that in the Ad-Mock group, the absorbance levels increased as the concentration of Ad-Mock decreased (Fig. 11). In the Ad-Cbx7 group, the absorbance level was highest when the Ad-Cbx7 level was medium, and lowest when the Ad-Cbx7 level was low. The possible explanation was that the MEF cells had reached the growth plateau when a low amount of Ad-Cbx7 was treated. As a result, the cells did not grow. In the CBX7 variant group, the absorbance levels did not change as much as the ad-Cbx7. However, it was clear to see that the absorbance level of CBX7 variant

was significantly higher than no treatment and ad-Mock group. The second MTT assay was conducted with 2%FBS. The result was consistent with the previous MTT assay with 10% FBS media result (Fig.12).

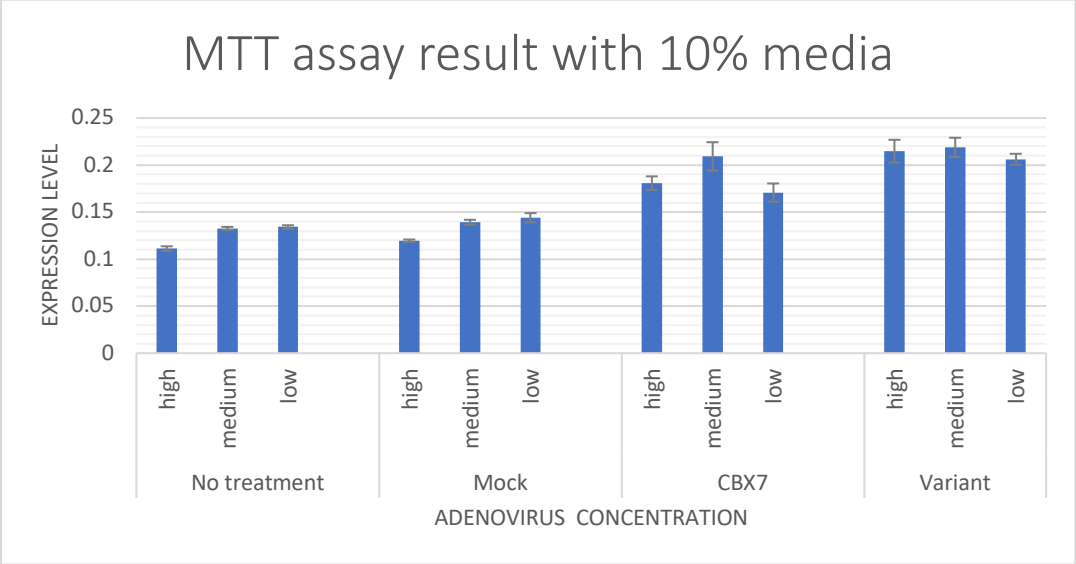

Figure 11. MTT assay result with 10% media. MEF cells in the 10% media were infected by ad-Mock, ad-Cbx7, and ad-Cbx7v. As the amount of Mock adenovirus decreased, the absorbance level increased in the ad-Mock group. As the amount of ad-Cbx7 and ad-Cbx7v decreased, the absorbance level did not change proportionally.

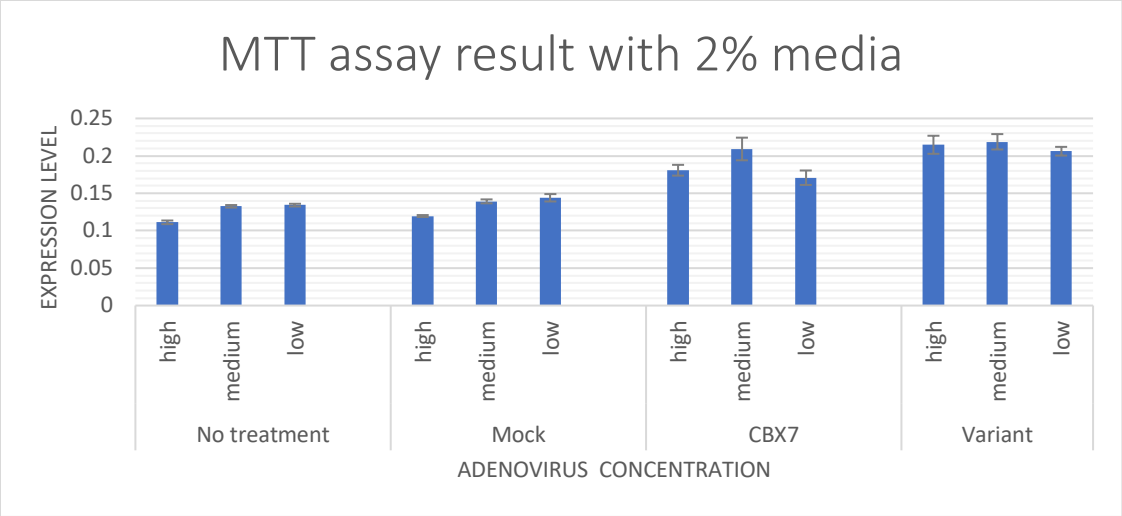

Figure 12. MTT assay result with 2% media. MEF cells in the 2% media were infected by ad-Mock, ad-Cbx7, and ad-Cbx7v. As the amount of Mock adenovirus decreased, the absorbance level increased in the ad-Mock group. As the amount of ad-Cbx7 and ad-Cbx7v decreased, the absorbance level did not change proportionally.

Real-time PCR showed the expression level of cell cycle markers

Other than checking the metabolic change, it was possible to exam the cell cycle markers such as Ccna1, Cccna2, Cccnb1 etc. Thus, rtPCR was conducted to check cell cycle marker gene expression level. The primary function of Ccna1 is to control meiosis at the G1/S (start) and G2/M (mitosis) transitions. Treating ad-Mock and ad-Cbx7, there was no obvious increase in Ccna1 gene expression level. However, after treating ad-Cbx7V, the Ccna1 gene expression level was much higher than other treatment groups (Fig.13). This result indicated that the *Cbx7* variant led to cell proliferation. Primary functions of Ccna2, Ccnb1 are similar to Ccna1. However, both the no treatment group and treatment groups led to a various degree of increasing Ccna2 and Ccnb1 expression (Fig. 14,15). Although Ccnb3 also has a similar function as Ccna1, the rtPCR result shows high Ccnb3 expression in the no treatment group but low expression in the treatment groups (Fig.15). The results of Ccnd1, Ccnd2, Ccnd 3 and Ccne2 expressions show a similar pattern as

the result of Ccna1 (Fig.17,18,19,20). There was a low expression level in the no treatment group and Ad-Mock group. In Ad-Cbx7 group, these gene expressions relatively increased.

When Ad-Cbx7 V was treated, these gene expressions drastically increased. The p16 expression level showed showed a high level of expression in both the no treatment and treatment group (Fig.21). The primary function of p15 is similar to that of p16. It acts as a tumor suppressor. The rt-PCR result of p15 also shows a similar pattern of expression level as the result of p16 (Fig.22). P27 controls the cell cycle progression at G1. It is as a cell cycle inhibitor protein because its major function is to stop or slow down the cell division cycle. The rt-PCR result of p27 shows there was low gene expression in the no treatment. As ad-Mock was treated, the gene expression level increase. As ad-Cbx7 and ad Cbx7 V were treated, the high p27 expression level was detected (Fig.23). ARF is also involved in cell cycle regulation by inhibiting the cell through the G1/S checkpoint of the cell cycle. The rt-PCR result of ARF was similar to the result of p27. There was low gene expression in the no treatment. As ad-Mock was treated, the gene expression level increased. As ad-Cbx7 and ad Cbx7 V were treated, high ARF expression level was detected (Fig.24).

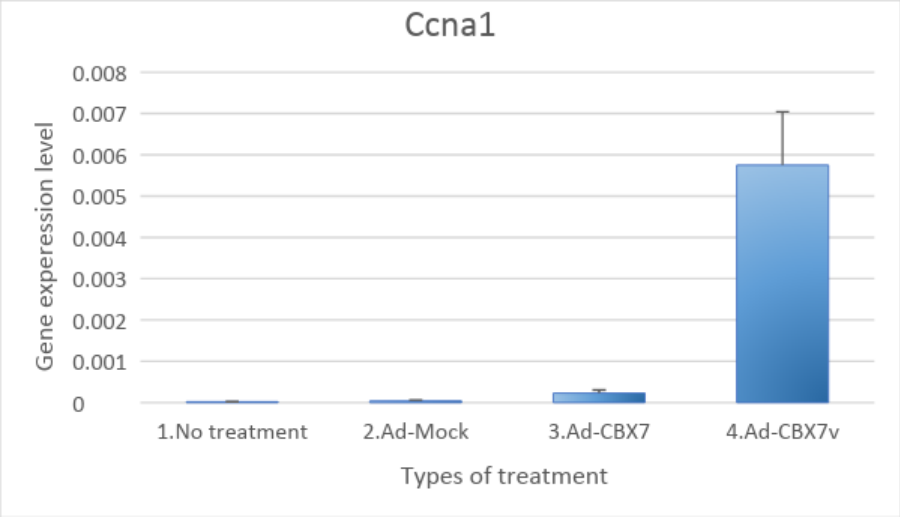

Figure 13. Real-time PCR result of Ccna1 gene expression. Both the no treatment and Ad-Mock treatment were control groups. There was almost no expression of Ccna1 gene in the control group. After treating Ad-Cbx7 and Ad-Cbx7V, the expression level of Ccna1 gene increased.

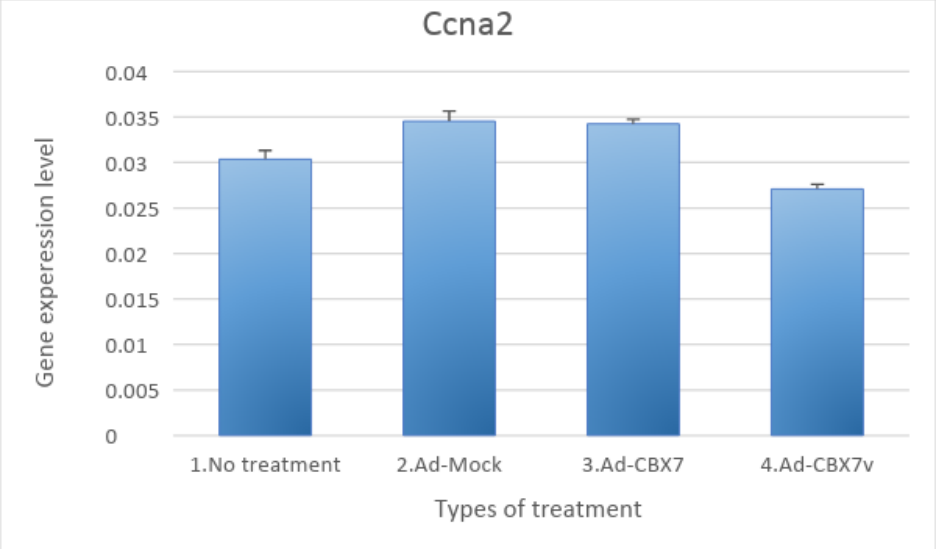

Figure 14. Real-time PCR result of Ccna2 gene expression. Both the no treatment and Ad-Mock treatment were control groups. There was increased expression of Ccna2 gene in the control group. After treating Ad-Cbx7 and Ad-Cbx7V to MEF cells, the expression level of Ccna2 gene increased.

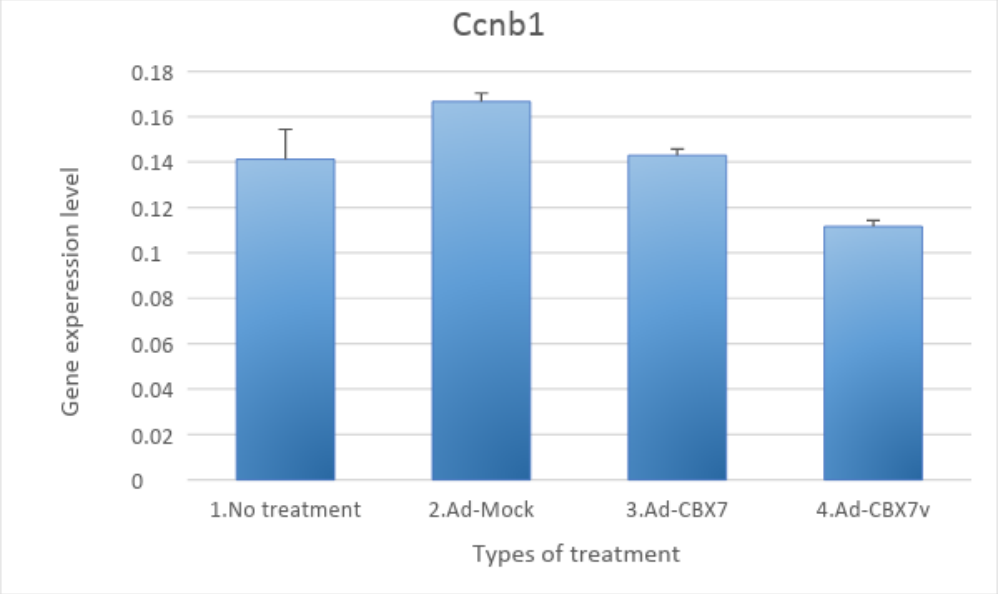

Figure 15. Real-time PCR result of Ccnb1 gene expression. Both the no treatment and Ad-Mock treatment were control groups. There were increased expressions of Ccnb1 gene in the control group. After treating Ad-Cbx7 and Ad-Cbx7V to MEF cells, the expression level of Ccnb1 gene increased but increased less than the control group.

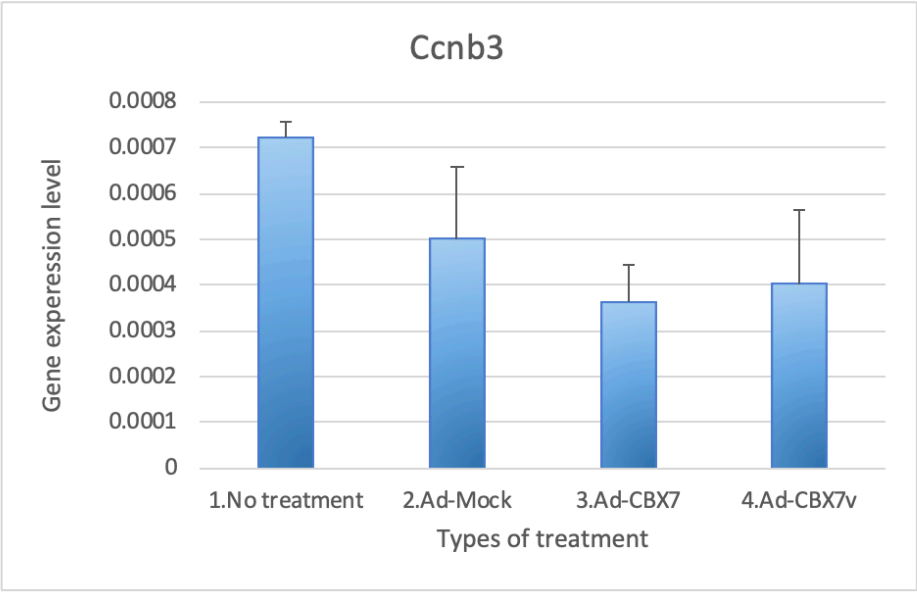

Figure 16. Real-time PCR result of Ccnb3 gene expression. Both the no treatment and Ad-Mock treatment were control groups. There were increased expressions of Ccnb1 gene in the control group. After treating Ad-Cbx7 and Ad-Cbx7V to MEF cells, the expression level of Ccnb3 gene slightly increased, but not increased as much as the control groups did.

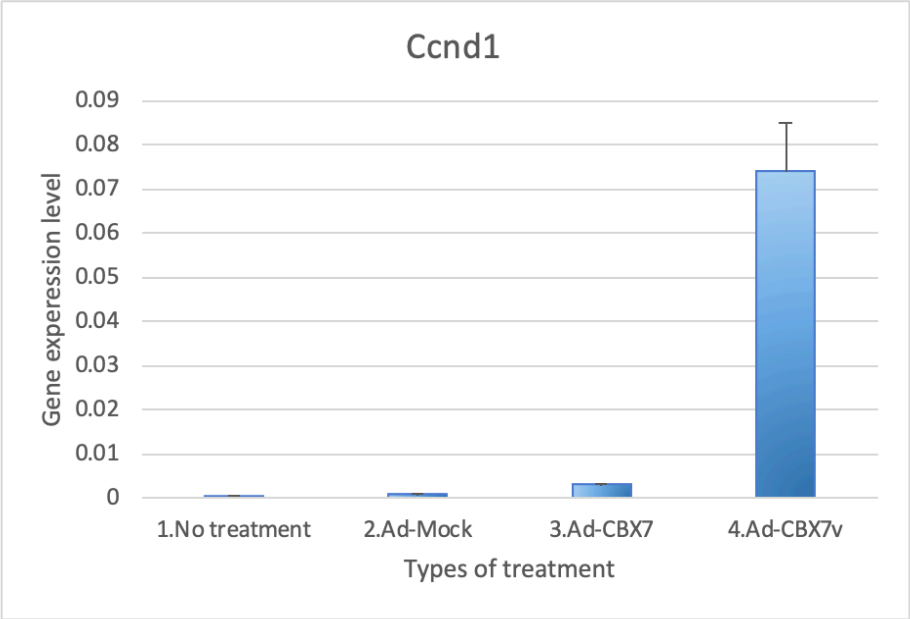

Figure 17. Real-time PCR result of Ccnd1 gene expression. Both the no treatment and Ad-Mock treatment were control groups. There was no expression of Ccnd1 gene in the control group. After treating Ad-Cbx7 and Ad-Cbx7V to MEF cells, the expression level of Ccnd3 gene increased.

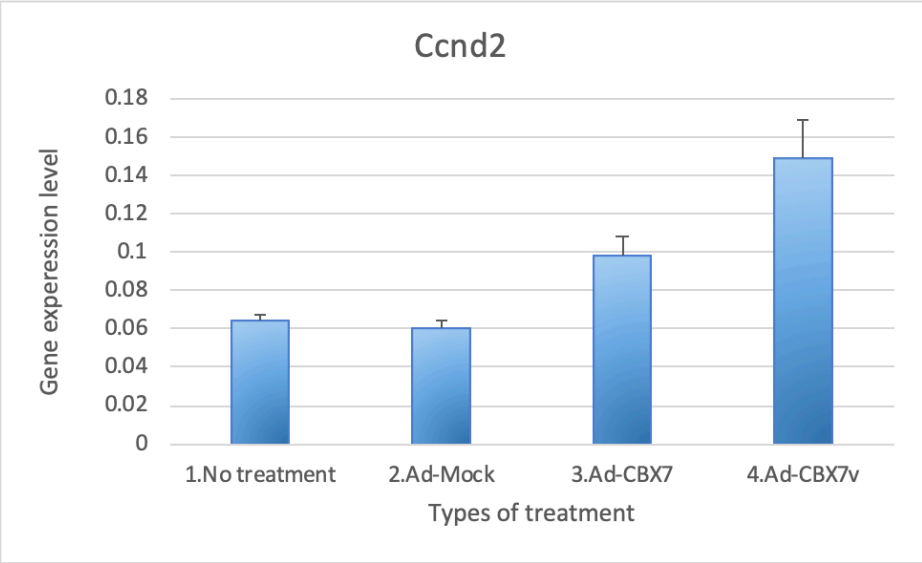

Figure 18. Real-time PCR result of Ccnd2 gene expression. Both the no treatment and Ad-Mock treatment were control groups. There were gene expressions of Ccnd2 gene in the control group. After treating Ad-Cbx7 and Ad-Cbx7V to MEF cells, the expression level of Ccnd3 gene increased.

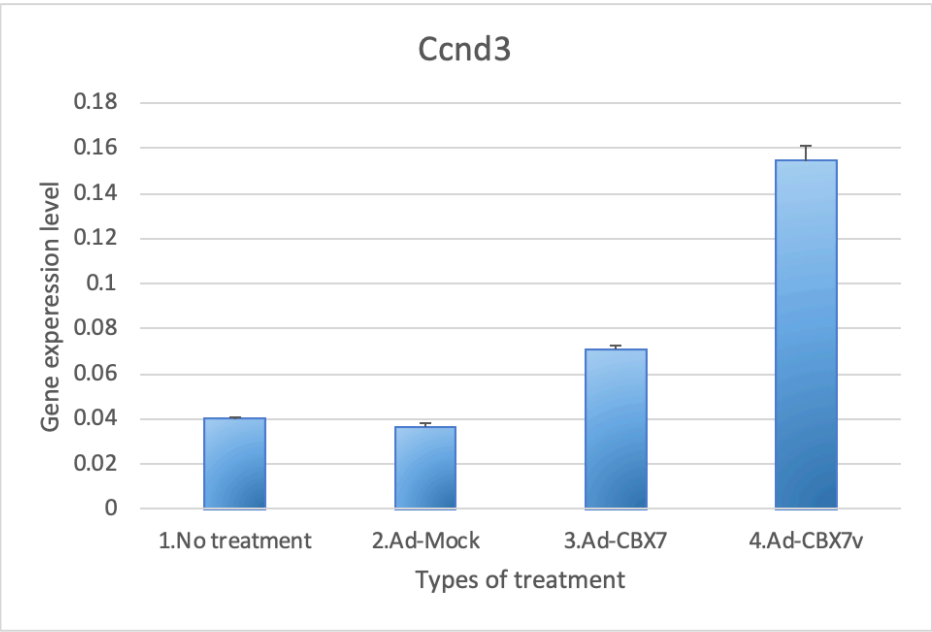

Figure 19. Real-time PCR result of Ccnd3 gene expression. Both the no treatment and Ad-Mock treatment were control groups. There were gene expressions of Ccnd3 gene in the control group. After treating Ad-Cbx7 and Ad-Cbx7V to MEF cells, the expression level of Ccnd3 gene increased.

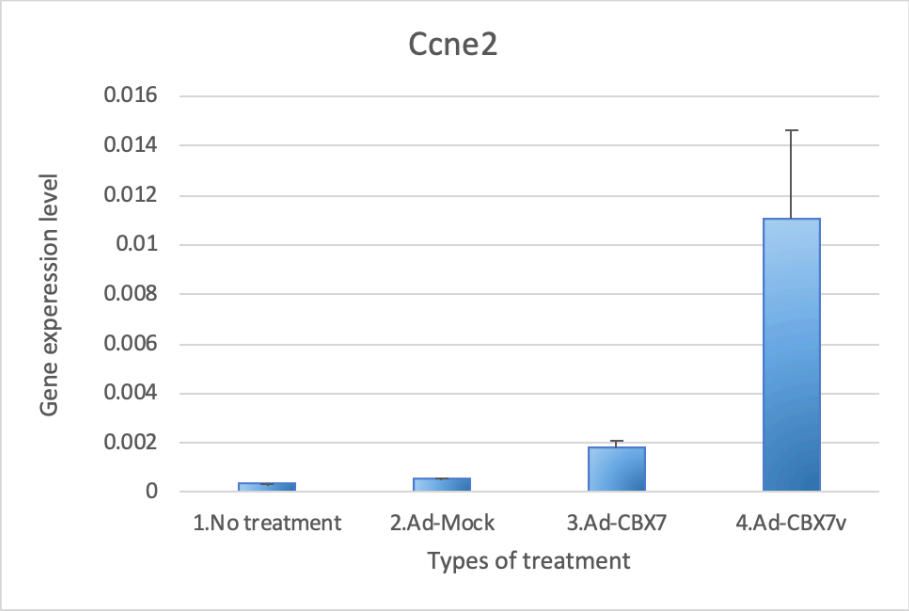

Figure 20. Real-time PCR result of Ccne2 gene expression. Both the no treatment and Ad-Mock treatment were control groups. There were minimum gene expressions of Ccne2 gene in the control group. After treating Ad-Cbx7 and Ad-Cbx7V to MEF cells, the expression level of Ccnd3 gene increased.

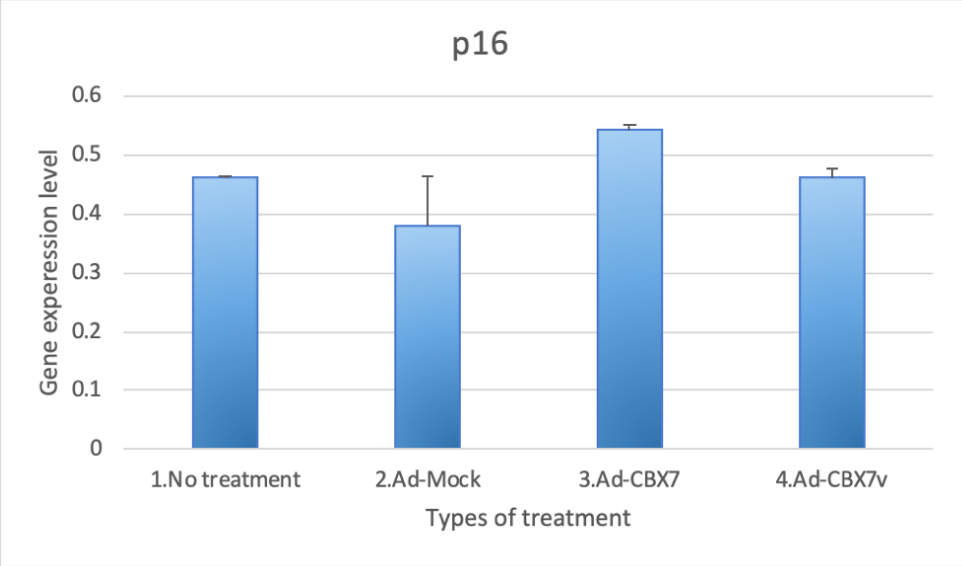

Figure 21. Real-time PCR result of p16 gene expression. Both the no treatment and Ad-Mock treatment were control groups. There were gene expressions of p16 gene in the control group. After treating Ad-Cbx7 and Ad-Cbx7V to MEF cells, the expression level of p16 gene relatively increased.

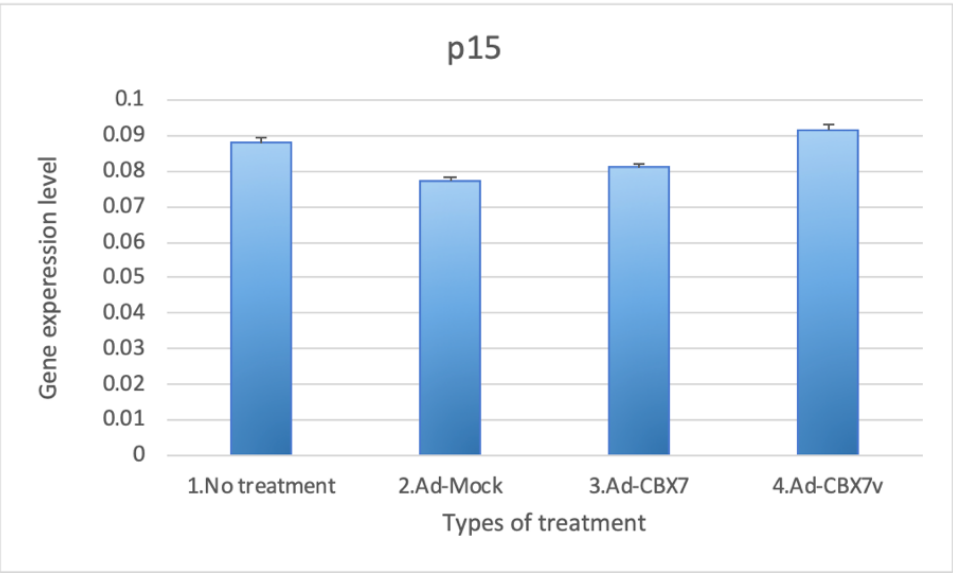

Figure 22. Real-time PCR result of p15 gene expression. Both the no treatment and Ad-Mock treatment were control groups. There were strong gene expressions of the p15 gene in the control group. After treating Ad-Cbx7 and Ad-Cbx7V to MEF cells, the expression levels of the p15 gene increased.

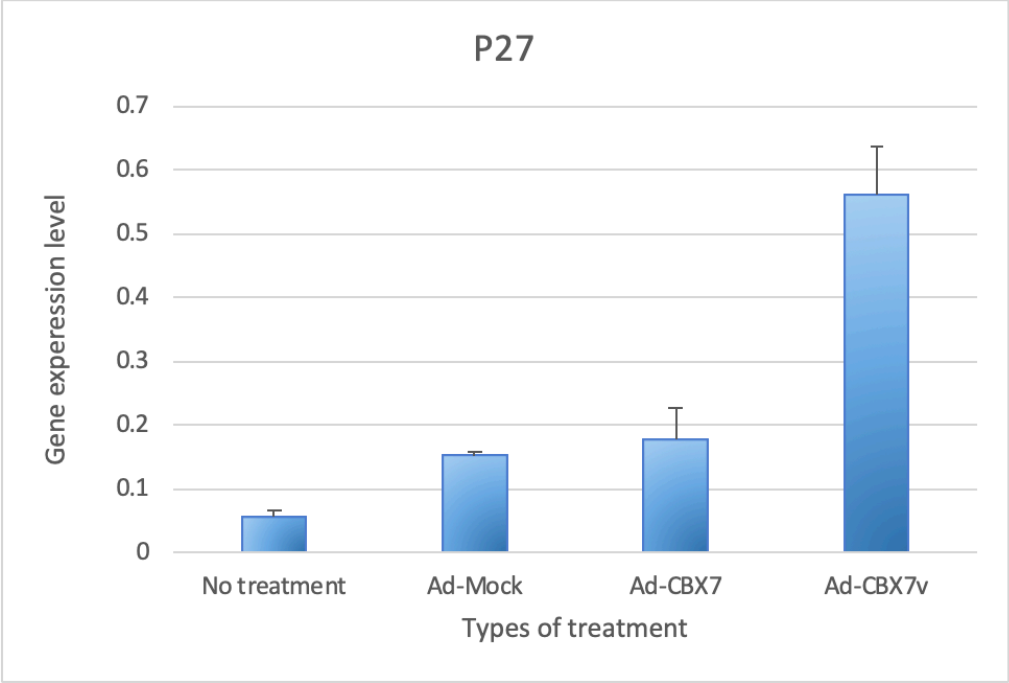

Figure 23. Real-time PCR result of p27 gene expression. Both the no treatment and Ad-Mock treatment were control groups. There were gene expressions of p27 gene in the control group. After treating Ad-Cbx7 and Ad-Cbx7V to MEF cells, the expression levels of p27 gene increased more than that of control group.

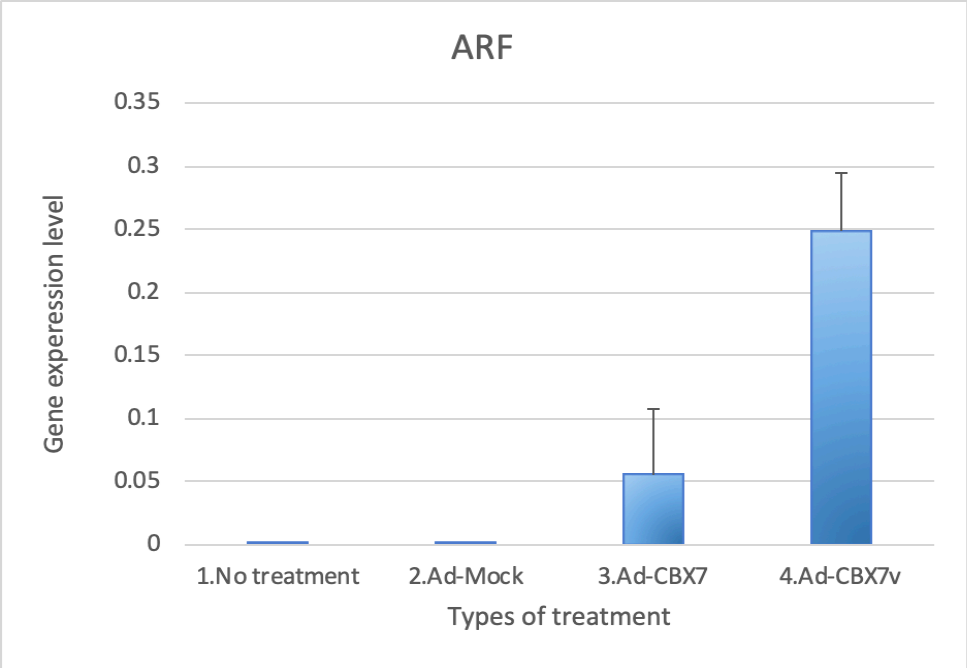

Figure 24. Real-time PCR result of ARF gene expression. Both No treatment and Ad-Mock treatment were control groups. There were almost no gene expressions of ARF gene in the control group. After treating Ad-Cbx7 and Ad-Cbx7V to MEF cells, the expression levels of ARF gene increased.

Discussion

The role of CBX7 in the regulation of cell growth and tumorigenesis is controversial. There is evidence that its overexpression causes tumor development, which indicates that CBX7 acts as an oncogene (22,23,24). However, the loss of CBX7 expression also correlates with highly malignant tumors (29,30,31). If we can address this issue: whether or not the CBX7 functions acts as a tumor suppressor, we can then create effective cancer treatments that specifically target CBX7. To tackle this problem, we used a strategy to verify the function of CBX7, which has two main components: molecular cloning and functional characterization assays.

In the first component, we discovered the Cbx7 variant gene and then successfully cloned it. Cbx7 mRNA was isolated from the newborn mouse fetal heart, and then its cDNA was generated using reverse transcriptase. A PCR amplification reaction was then carried out. PCR results led to the discovery of the Cbx7 transcript variant gene in the mouse fetal heart (Fig 3). Then, we amplified the Cbx7 variant gene. The Cbx7 variant gene was effectively ligated into the TA cloning pCR2.1 TOPO vector. The positive insertion was verified through the Blue-White screening (Fig 4). We also used a restriction enzyme called EcoR1 to digest pCR2.1-TOPO plasmid and results confirmed that the Cbx7 variant gene was successfully inserted into the plasmid (Fig 5). The success of Cbx7 variant cloning allowed us to conduct more experiments to compare its functional mechanism with the Cbx7 gene.

After we accomplished cloning, we sent Cbx7 variant off to be sequenced. Sequencing results indicated that the Cbx7 and Cbx7 transcript variant have very similar sequence makeups (Fig 6), with the addition of exon 5 in the variant. This difference might lead to Cbx7 and Cbx7 transcript variant to have opposite functions: one acts as an oncogene, the other acts as a tumor suppressor. Therefore, we hypothesized that the *Cbx7* variant gene that contains the extra exon 5 region is the controlling factor in whether the *Cbx7* gene will become an oncogene or tumor suppressor.

In the second component, we generated recombinant adenovirus for the gain of function (GOF) analyses. The recombinant adenovirus that overexpresses *Cbx7* and its variant gene were amplified in HEK293 cells and titrated (Fig 7,8,9). After infecting MEF cells with recombinant adenovirus, we were able to perform the western blot analysis to check the CBX7 variant protein expression level in MEF cells (Fig 10). The western blot results directly showed that Cbx7 and its variant were two separate transcripts because their protein expression level and size were different.

In addition, we conducted proliferation assays to assess the metabolic activity in a cell, and rt-PCR to exam the cell cycle regulatory gene expression.

After analyzing current data, we could not draw a conclusion as to whether or not CBX7 and its variant have an opposing role from one other. There were several aspects of MTT assay and rt-PCR that could possibly have negatively impacted the experiment results. First, the MEF cell line was contaminated such that cells were not healthy enough to be infected by recombinant adenovirus to incorporate the target gene. Therefore, inconclusive MTT results were collected. This error might be resolved by changing to another cell line. Secondly, high error bars with rtPCR were possibly the result of pipetting error and cross-contamination. This may be resolved by improving pipetting techniques. Third, the titration method was not precise enough to show the true concentration of adenovirus because it was a rating-based method that required the estimation of the cell survival rate. This may be overcome by using the cell-counting titration method to improve upon precision and accuracy. Treating unequal amounts of adenovirus could lead to inconclusive results when conducting an MTT assay. Finally, MEF cells can often form cell clusters that potentially skew the MTT assay result as cell clusters lead to a higher number of cells in each well. More cells in the well might suggest higher metabolic activity. Therefore, the MTT assay result may not be reliable. This may be resolved by filtering cells before conducting the assay to remove cell cluster.

In conclusion, the discovery of the Cbx7 transcript variant can possibly explain the opposing roles of the CBX7 protein. Successful cloning of the Cbx7 variant enables us to repeat functional characterization assays such as MTT assays and rt-PCR. Although these assays may not have led to a reliable conclusion, it is still possible to obtain conclusive results after resolving the aforementioned issues. Therefore, we plan to repeat the proliferation assays and perform real-time PCR again to further address the functional role of CBX7 and CBX7 variant.

References

1. Hanahan D, Weinberg RA. The hallmarks of cancer. Cell. 2000;100(1):57-70.
2. Futreal PA, Coin L, Marshall M, Down T, Hubbard T, Wooster R, et al. A census of human cancer genes. Nature reviews Cancer. 2004;4(3):177-83.
3. Baylin SB, Herman JG. DNA hypermethylation in tumorigenesis: epigenetics joins genetics. Trends in genetics : TIG. 2000;16(4):168-74.
4. Jacobs JJ, Kieboom K, Marino S, DePinho RA, van Lohuizen M. The oncogene and Polycomb-group gene bmi-1 regulates cell proliferation and senescence through the ink4a locus. Nature. 1999;397(6715):164-8.
5. Jones PA. DNA methylation and cancer. Oncogene. 2002;21(35):5358-60.
6. Pasini D, Bracken AP, Helin K. Polycomb group proteins in cell cycle progression and cancer. Cell cycle (Georgetown, Tex). 2004;3(4):396-400.
7. Francis NJ, Kingston RE. Mechanisms of transcriptional memory. Nature reviews Molecular cell biology. 2001;2(6):409-21.
8. Icard P, Lincet H. A global view of the biochemical pathways involved in the regulation of the metabolism of cancer cells. Biochimica et biophysica acta. 2012;1826(2):423-33.
9. Greene ND, Stanier P, Moore GE. The emerging role of epigenetic mechanisms in the etiology of neural tube defects. Epigenetics. 2011;6(7):875-83.
10. Holec S, Berger F. Polycomb group complexes mediate developmental transitions in plants. Plant physiology. 2012;158(1):35-43.
11. Park IK, Qian D, Kiel M, Becker MW, Pihalja M, Weissman IL, et al. Bmi-1 is required for maintenance of adult self-renewing haematopoietic stem cells. Nature. 2003;423(6937):302-5.

12. Park IK, Morrison SJ, Clarke MF (January 2004). Bmi1, stem cells, and senescence regulation. The Journal of Clinical Investigation. 113 (2): 175–9.
13. Bansal N, Bartucci M, Yusuff S, Davis S, Flaherty K, Huselid E, et al. BMI-1 Targeting Interferes with Patient-Derived Tumor-Initiating Cell Survival and Tumor Growth in Prostate Cancer. Clinical cancer research : an official journal of the American Association for Cancer Research. 2016;22(24):6176-91.
14. Molofsky AV, He S, Bydon M, Morrison SJ, Pardal R (June 2005). Bmi-1 promotes neural stem cell self-renewal and neural development but not mouse growth and survival by repressing the p16Ink4a and p19Arf senescence pathways. Genes & Development. 19 (12): 1432–7.
15. Popov N, Gil J (2010). Epigenetic regulation of the INK4b-ARF-INK4a locus: in sickness and in health. Epigenetics. 5 (8): 685–90.
16. Swalm BM, Knutson SK, Warholic NM, Jin L, Kuntz KW, Keilhack H, et al. Reaction coupling between wild-type and disease-associated mutant EZH2. ACS chemical biology. 2014;9(11):2459-64.
17. Wu Y, Hu H, Zhang W, Li Z, Diao P, Wang D, et al. SUZ12 is a novel putative oncogene promoting tumorigenesis in head and neck squamous cell carcinoma. Journal of cellular and molecular medicine. 2018;22(7):3582-94.
18. Ku M, Koche RP, Rheinbay E, Mendenhall EM, Endoh M, Mikkelsen TS, Presser A, Nusbaum C, Xie X, Chi AS, Adli M, Kasif S, Ptaszek LM, Cowan CA, Lander ES, Koseki H, Bernstein BE (October 2008). Genomewide analysis of PRC1 and PRC2 occupancy identifies two classes of bivalent domains. PLoS Genetics. 4 (10):
19. Yuan W, Wu T, Fu H, Dai C, Wu H, Liu N, et al. Dense chromatin activates Polycomb repressive complex 2 to regulate H3 lysine 27 methylation. Science (New York, NY). 2012;337(6097):971-5.

20. Joseph H. A. Vissers, Maarten van Lohuizen, Elisabetta Citterio (2012). The emerging role of Polycomb repressors in the response to DNA damage J Cell Sci 125: 3939-3948.
21. Pallante, P., Forzati, F., Federico, A., Arra, C., & Fusco, A. (2015). Polycomb protein family member CBX7 plays a critical role in cancer progression. *American journal of cancer research*, *5*(5), 1594-601.
22. Gil J, Bernard D, Martinez D, Beach D. Polycomb CBX7 has a unifying role in cellular lifespan. Nat Cell Biol. 2004;6(1):67-72.
23. Ma RG, Zhang Y, Sun TT, Cheng B. Epigenetic regulation by polycomb group complexes: focus on roles of CBX proteins. J Zhejiang Univ Sci B. 2014;15(5):412-28.
24. Scott CL, Gil J, Hernando E, Teruya-Feldstein J, Narita M, Martinez D, Visakorpi T, Mu D, Cordon-Cardo C, Peters G, Beach D, Lowe SW. Role of the chromobox protein CBX7 in lymphomagenesis. Proc Natl Acad Sci U S A. 2007;104:5389–5394.
25. Wu W, Zhou X, Yu T, Bao Z, Zhi T, Jiang K, et al. The malignancy of miR-18a in human glioblastoma via directly targeting CBX7. American journal of cancer research. 2017;7(1):64-76.
26. Cacciola NA, Sepe R, Forzati F, Federico A, Pellecchia S, Malapelle U, De Stefano A, Rocco D, Fusco A, Pallante P. Restoration of CBX7 expression increases the susceptibility of human lung carcinoma cells to irinotecan treatment. Naunyn-Schmiedeberg's archives of pharmacology. 2015
27. Pallante P, Forzati F, Federico A, Arra C, Fusco A. Polycomb protein family member CBX7 plays a critical role in cancer progression. *Am J Cancer Res*. 2015;5(5):1594–1601. Published 2015 Apr 15.
28. Pallante P, Terracciano L, Carafa V, Schneider S, Zlobec I, Lugli A, Bianco M, Ferraro A, Sacchetti S, Troncone G, Fusco A, Tornillo L. The loss of the CBX7 gene expression

represents an adverse prognostic marker for survival of colon carcinoma patients. European journal of cancer. 2010;46:2304–2313.

29. Karamitopoulou E, Pallante P, Zlobec I, Tornillo L, Carafa V, Schaffner T, Borner M, Diamantis I, Esposito F, Brunner T, Zimmermann A, Federico A, Terracciano L, Fusco A. Loss of the CBX7 protein expression correlates with a more aggressive phenotype in pancreatic cancer. European journal of cancer. 2010;46:1438–1444.
30. Zhang XW, Zhang L, Qin W, et al. Oncogenic role of the chromobox protein CBX7 in gastric cancer. *J Exp Clin Cancer Res*. 2010;29(1):114. Published 2010 Aug 19. doi:10.1186/1756-9966-29-114
31. Forzati F, Federico A, Pallante P, Abbate A, Esposito F, Malapelle U, et al. CBX7 is a tumor suppressor in mice and humans. J Clin Invest. 2012;122(2):612-23.
32. Ni S, Wang H, Zhu X, et al. CBX7 suppresses cell proliferation, migration, and invasion through the inhibition of PTEN/Akt signaling in pancreatic cancer. *Oncotarget*. 2016;8(5):8010–8021. doi:10.18632/oncotarget.14037
33. Forzati F, Federico A, Pallante P, Colamaio M, Esposito F, Sepe R, et al. CBX7 gene expression plays a negative role in adipocyte cell growth and differentiation. Biol Open. 2014;3(9):871-9.
34. Federico A, et al. Chromobox protein homologue 7 protein, with decreased expression in human carcinomas, positively regulates E-cadherin expression by interacting with the histone deacetylase 2 protein. *Cancer Res.* 2009;69(17):7079–7087.
35. Sherr CJ (September 2006). Divorcing ARF and p53: an unsettled case. *Nat. Rev. Cancer*. **6** (9): 663–73. doi:10.1038/nrc1954. PMID 16915296.
36. Nobori T, Miura K, Wu DJ, Lois A, Takabayashi K, Carson DA (April 1994). Deletions of the cyclin-dependent kinase-4 inhibitor gene in multiple human cancers. *Nature*. **368** (6473): 753–6. doi:10.1038/368753a0. PMID 8152487

37. Pan FP, Zhou HK, Bu HQ, et al. Emodin enhances the demethylation by 5-Aza-CdR of pancreatic cancer cell tumor-suppressor genes P16, RASSF1A and ppENK. *Oncol Rep*. 2016;35(4):1941–1949. doi:10.3892/or.2016.4554